

# Adaptive divergence despite low effective population size in a peripherally isolated population of the pygmy rabbit, *Brachylagus idahoensis*

Nathan W. Byer<sup>1</sup>  | Matthew L. Holding<sup>1</sup> | Miranda M. Crowell<sup>1</sup> | Todd W. Pierson<sup>2</sup> | Thomas E. Dilts<sup>1</sup> | Eveline S. Larrucea<sup>3</sup> | Kevin T. Shoemaker<sup>1</sup> | Marjorie D. Matocq<sup>1</sup>

<sup>1</sup>Department of Natural Resources and Environmental Science, University of Nevada–Reno, Reno, Nevada, USA

<sup>2</sup>Department of Ecology, Evolution, and Organismal Biology, Kennesaw State University, Kennesaw, Georgia, USA

<sup>3</sup>Lemon Canyon Ranch, Sierraville, California, USA

#### Correspondence

Nathan W. Byer, Department of Natural Resources and Environmental Science, University of Nevada–Reno, Reno, NV, USA.

Email: nathanbyer1@gmail.com

#### Funding information

Nevada Department of Wildlife; U.S. Fish and Wildlife Service; Great Basin Landscape Conservation Cooperative; Greater Hart-Sheldon Fund; National Science Foundation, Grant/Award Number: OIA-1826801

## Abstract

Local adaptation can occur when spatially separated populations are subjected to contrasting environmental conditions. Historically, understanding the genetic basis of adaptation has been difficult, but increased availability of genome-wide markers facilitates studies of local adaptation in non-model organisms of conservation concern. The pygmy rabbit (*Brachylagus idahoensis*) is an imperiled lagomorph that relies on sagebrush for forage and cover. This reliance has led to widespread population declines following reductions in the distribution of sagebrush, leading to geographic separation between populations. In this study, we used >20,000 single nucleotide polymorphisms, genotype-environment association methods, and demographic modeling to examine neutral genetic variation and local adaptation in the pygmy rabbit in Nevada and California. We identified 308 loci as outliers, many of which had functional annotations related to metabolism of plant secondary compounds. Likewise, patterns of spatial variation in outlier loci were correlated with landscape and climatic variables including proximity to streams, sagebrush cover, and precipitation. We found that populations in the Mono Basin of California probably diverged from other Great Basin populations during late Pleistocene climate oscillations, and that this region is adaptively differentiated from other regions in the southern Great Basin despite limited gene flow and low effective population size. Our results demonstrate that peripherally isolated populations can maintain adaptive divergence.

#### KEY WORDS

coalescent simulations, detoxification, landscape genomics, local adaptation, pygmy rabbits

## 1 | INTRODUCTION

Identifying how neutral and selective processes determine patterns of biological diversity remains one of the grand challenges of evolutionary biology (Heywood, 1991; Loiselle et al., 1995; Rousset, 2001; Vekemans & Hardy, 2004). Even in species that are nearly continuously distributed, limitations to dispersal will typically result

in genetic patterns of isolation by distance. In addition, when geographic or environmental barriers exist, spatial connectivity may be reduced further, limiting gene flow, increasing genetic drift, and ultimately leading to genetic discontinuities across the landscape (Coulon et al., 2004; Cushman et al., 2006; Lowe & Allendorf, 2010). When populations separated in space are subjected to contrasting environmental conditions and selective pressures, genetic

differentiation may also reflect local adaptation (Hanski et al., 2011; Kawecki & Ebert, 2004; Sork et al., 2010). Given sufficient time, interactions between genetic drift and directional selection may give rise to substantial within-species adaptive genetic differentiation across spatially separated populations (Araneda et al., 2016; Mable, 2019). However, the extent to which actively declining populations can maintain adaptive genetic variation requires additional study with high-resolution genetic data sets (Hoffmann & Willi, 2008; Schoville et al., 2011).

Given the scope of declines in biodiversity throughout the late 20th and early 21st centuries, documenting spatial patterns in genetic variation has become central to conservation and management (Hoffmann & Willi, 2008; Lowe & Allendorf, 2010). As humans fragment existing habitat, wildlife populations become more isolated, reducing genetic variation within populations, and increasing genetic divergence among populations (Gibbs, 2001; Keyghobadi, 2007; Templeton et al., 1990; Young et al., 1996). Although reductions in gene flow may facilitate local adaptation (Räsänen & Hendry, 2008; Tigano & Friesen, 2016), habitat fragmentation often reduces effective population sizes to a point where genetic drift is the dominant evolutionary force, thus reducing potential for local adaptation in isolated populations and the probability of species persistence (Sultan & Spencer, 2002; Tigano & Friesen, 2016).

While identifying the genetic basis of ecological adaptations will remain a challenge for decades to come, major technological and analytical advances are pushing this area of inquiry forward (Fitzpatrick & Keller, 2015; Larsen & Matocq, 2019; Manel et al., 2010; Sork et al., 2013). However, for most wild non-model systems, functional genomic data needed to make a priori predictions still do not exist, and sparse genome-wide data coupled with statistical limitations make it difficult to infer directional selection post hoc (Manel et al., 2010; Schoville et al., 2011; Sork et al., 2013). Since adaptive genetic diversity is shaped by both genetic drift and selection, adaptive genetic variation may display complex and unpredictable patterns relative to neutral expectations (Hoffmann & Willi, 2008; Holderegger et al., 2006; Meyer-Lucht et al., 2016; Sork et al., 2016). Thus, studies that hope to disentangle adaptive and neutral genetic variation must exercise caution in choice of molecular markers by either leveraging a priori knowledge of neutral and adaptive roles associated with gene regions of choice or discriminating between adaptive and neutral loci post hoc (Manel et al., 2010; Savolainen et al., 2013; Schoville et al., 2011; Sork et al., 2016). Nonetheless, by coupling functional genomic information from model systems with new methods of analysis that integrate genomic data with remotely sensed environmental data, we can generate hypotheses about potential associations between genotype and environment.

These advances have been particularly important in allowing for detailed investigation of local adaptation in non-model species, including those of conservation importance (Kohn et al., 2006; Savolainen et al., 2013; Segelbacher et al., 2010; Sork et al., 2013). The pygmy rabbit (*Brachylagus idahoensis*), listed as a species of special concern in California and Nevada (Larrucea et al., 2018), is a sagebrush specialist that relies on big sagebrush (*Artemisia*

*tridentata*) for both diet and shelter (Gabler et al., 2001; Katzner & Parker, 1997; White et al., 1982). Although the range of this species encompasses much of the Great Basin of western North America, reduction in the distribution of big sagebrush caused by overgrazing, invasion of exotic grasses, and changes in fire regimes has severely limited the distribution of suitable habitat (Crawford et al., 2010; Gabler et al., 2001; Weiss & Verts, 1984), resulting in pygmy rabbit population declines and a pressing need for increased conservation efforts (Crawford et al., 2010; Crowell et al., 2020; Dobler & Dixon, 1990; Larrucea & Brussard, 2008).

Studies of genetic diversity in the pygmy rabbit have revealed low to moderate genetic differentiation between populations and pervasive isolation-by-distance in several geographic regions (Estes-Zumpf et al., 2010; Larrucea et al., 2018; Warheit, 2001). In the southern portion of its range, Larrucea et al. (2018) documented marked differentiation between pygmy rabbit populations in the Mono Basin of California and populations in the southern Great Basin ( $F_{ST} = 0.14$ –0.31, average 0.22). Byer et al. (2021) showed that population genetic structure, as measured by microsatellite variation, is strongly correlated to the distribution of sagebrush (Figure 1). While range-wide studies of genetic variation have not been conducted, strong divergence between populations in Oregon and Washington ( $F_{ST} = 0.29$  to 0.32; Elias et al., 2013; Larrucea et al., 2018; Warheit, 2001) suggest relatively low gene flow between these regions, although the timescale of this differentiation remains uncertain. All recent studies of pygmy rabbits have used microsatellite markers, which generally have less power to detect genetic differentiation than SNP data sets (Fischer et al., 2017; Hauser et al., 2011) and do not address adaptive genetic variation due to their selective neutrality (Manel et al., 2010).

Here, we present the first application of single nucleotide polymorphisms (SNPs) to characterize neutral and adaptive spatial genetic structure across the southern range of the pygmy rabbit by: (i) identifying loci potentially under directional selection, (ii) characterizing both neutral and adaptive genetic variation throughout the study area, and (iii) contextualizing patterns of genetic divergence in light of demographic history. We made several predictions. First, since previous studies of sagebrush obligates have found signatures of directional selection at genes associated with metabolism of plant secondary compounds (PSCs), we predicted that we would detect a signature of selection in genes associated with detoxification (Zimmerman et al., 2019). Second, we predicted that adaptive genetic divergence should correspond to ecological differences across the study region, particularly along climatic gradients. Third, given documented subdivision between Mono Basin and other Great Basin populations (Larrucea et al., 2018), we expected our demographic modeling would show the deepest time of divergence between the Mono Basin and other study regions, indicating prolonged isolation of this region. Overall, we expected that pygmy rabbit population genetic structure across this portion of the range would be characterized by broad-scale patterns of divergence largely reflective of their biogeographic history, coupled with patterns of neutral and adaptive divergence along current environmental gradients.

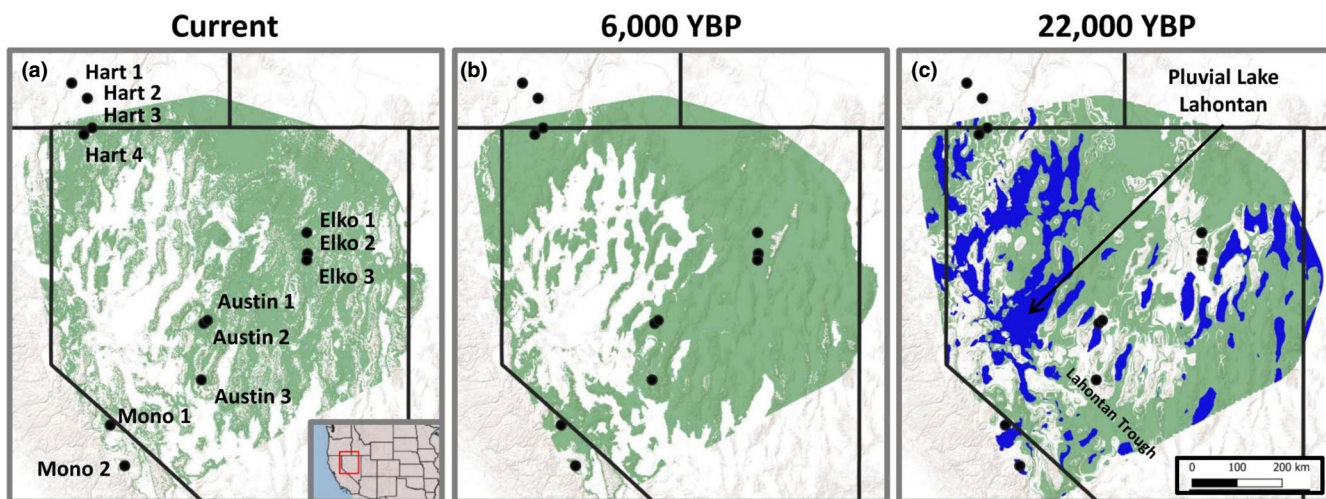


**FIGURE 1** Location of pygmy rabbit sampling localities (black dots), labelled by region (Austin, Elko, Hart, or Mono). (a) Present-day sagebrush distribution shown in green. (b) Projections of sagebrush distribution in the mid-Holocene (6000 years before present, or YBP) based on hind-casted distribution models of sagebrush (Byer et al., 2021). (c) Projections of sagebrush distribution in the late Pleistocene (22,000 YBP), with the footprint of pluvial lakes in blue. Modified from Byer et al. (2021) [Colour figure can be viewed at [wileyonlinelibrary.com](http://wileyonlinelibrary.com)]

## 2 | MATERIALS AND METHODS

### 2.1 | Field sampling, tissue sampling, and sequencing

We live-trapped at 18 localities in four core sampling regions (Austin, Elko, Hart-Sheldon, and Mono Basin) across the southern Great Basin (Figure 1) from 2016–2019, as described in Crowell et al. (2020). Briefly, we captured pygmy rabbits at active burrows using burlap-covered Tomahawk live traps. We documented sex, age, and reproductive status for each animal, and took a small ear biopsy (3 mm diameter) from each individual and stored the tissue in 95% ethanol at ambient temperature before long-term storage at  $-20^{\circ}\text{C}$ . We then extracted and quantified DNA concentrations for all samples, and we proceeded with preparation of 3RAD libraries following Bayona-Vásquez et al. (2019). See Supporting Information S1 for more details on DNA extraction and sequencing.

Following sequencing, we used *IPYRAD* v0.9.42 for *de novo* assembly and SNP discovery, producing a data set of 35,677 loci and 354,946 SNPs across 536 individuals with 7.5% missing data (Eaton & Overcast, 2020). This data set was filtered further using package *DARTR* in R version 3.6.1 (Gruber et al., 2018; R Core Team, 2020), producing a data set of 21,379 SNPs across 515 individuals; after dropping sampling localities with fewer than five individuals, our final sample size was 503 individuals across 12 sampling localities (see Supporting Information S1 for more details on *de novo* assembly, SNP discovery, and filtering). These samples were distributed across all years of sampling, with 103 in 2016, 209 in 2017, 161 in 2018, and 30 in 2019. This final data set ( $F_{ST} = 0.081$ ,  $F_{IS} = 0.020$ ,  $H_O = 0.253$ ) was used for all further analyses.

### 2.2 | Identification of outlier SNPs

We used three approaches to identify outlier loci that may be subject to directional selection and to separate our data set into putatively neutral and outlier subsets. We first used a principal components analysis (PCA) to detect outlier SNPs using the package *PCADAPT* in R (Luu et al., 2017). This method decomposes genetic variation into principal components (PCs), after which SNPs that are particularly influential in shaping genetic differentiation along each component are identified. We ran an initial PCA with 10 PCs and inspected variance explained by each PC using screeplots; after selecting the first several PCs that explained the most variance, we computed test statistics, adjusted these test statistics using a Bonferroni procedure, and used a false discovery rate (FDR) of 0.05 to control for false positives (Luu et al., 2017; Rödin-Mörch et al., 2019).

Our second approach used latent factors to account for coarse-scale population structure documented in previous studies (representing divergence between the Mono Basin and other Great Basin populations; Larrucea et al., 2018) and identified loci differentiated upon simplified environmental axes using latent factor mixed models (LFMM) in the packages *LFMM* and *LEA* in R (Frichot & François, 2015; Frichot et al., 2013). First, in order to eliminate missing data, we imputed any N/A values in our genetic matrix with the most common value at each SNP across all individuals ([https://popgen.nescent.org/2018-03-27\\_RDA\\_GEA.html](https://popgen.nescent.org/2018-03-27_RDA_GEA.html)). Given low proportions of missing data, we did not expect that this imputation method would impact downstream analyses; to verify this, we also explored two alternate imputation strategies: (i) imputing all missing data as homozygotes for the major allele (imputing 0 for all genotypes), and (ii) imputing all missing data as heterozygotes (imputing 1 for all genotypes). Neither of these settings appeared to visually alter patterns in multivariate genotypic space. Next, we selected a suite of land

cover, topographic, soil, and climate covariates that were previously identified as influential in species distribution models for this species (Dilts & Shoemaker, 2020); see Supporting Information S2 for details on these layers), and sampled covariates for each individual. We grouped these variables into PCs using function `rda` in package `VEGAN` (Dixon, 2003); as with `PCADAPT`, we inspected screeplots and proportions of variance explained by each axis to select the total number of environmental PCs to include in the analysis. We then used these PCs as fixed effects in downstream analyses. Given previous support from microsatellite analyses for a two-cluster solution, with one cluster encompassing the Mono Basin and the other encompassing remaining Great Basin populations (Larrucea et al., 2018), we chose to use two latent factors; although higher values of  $K$  were ultimately indicated from downstream clustering analyses (see below), initial tests of values of  $K$  between 4 and 7 did not appear to substantially alter the number of outliers detected. We then ran the Gibbs sampler with  $K = 2$  for 4000 iterations, following a burnin of 2000 iterations, and replicated each run three times. We ran this procedure separately for each PC, and we combined median z-scores for each PC-specific run. Finally, we adjusted  $p$ -values by a genomic inflation factor (GIF), and we used a FDR of 0.05 to control for false positives.

Finally, our third approach used partial redundancy analysis (pRDA), an ordination-based approach that controls for spatial structure in genetic differentiation and identifies outliers based on scores along environmental axes. While a number of Genotype-Environment Association (GEA) approaches exist, several recent studies have suggested advantages of redundancy analysis, including: (i) it has similar power to detect outlier loci as other approaches while minimizing false positive rates, and (ii) constrained redundancy analysis allows for identification of selective gradients in environmental variables (Capblancq et al., 2018; Forester et al., 2016, 2018; Sork et al., 2016). We used the same imputed data set as applied above. The same variables used for LFMM were used for pRDA analyses as fixed effects, and additive effects of latitude and longitude were included as conditioning factors to describe geographic structure in genetic variation. We assessed overall pRDA significance and significance of each pRDA axis using permutation tests with 9999 permutations and  $\alpha = 0.05$ , and ordination plots were then used to depict multivariate relationships. Analogous to the previous two approaches, we then inspected the proportion of variance explained by each constrained axis, assessed significance of the first five axes using permutation tests with 9999 permutations, and we calculated scores for each SNP along each significant axis (up to three axes). We retained outliers that were outside of three standard deviations from the mean SNP loading along each axis. Outliers detected by `PCADAPT`, LFMM, and pRDA were combined into a single data set that we refer to as our outlier data set. Although fitness associations would be necessary to confirm the role of outliers in evolutionary adaptation and the adaptive value of loci may shift across space and time (Hoffmann & Sgro, 2011; Schoville et al., 2011), we refer to variation in these outliers as “putatively adaptive”. We combined any SNPs not included in this outlier data set and hereafter refer this as our “neutral” data set.

To annotate loci containing outlier SNPs for functional roles, we first filtered the original list of assembled loci exported from `IPYRAD` to only include SNPs in our outlier data set. We converted these sequences into `FASTA` format and used a batch run in online `BLAST` to query this data set against the nucleotide database using `MEGABLAST` (Altschul et al., 1990). We filtered `BLAST` hits to  $E$ -values less than or equal to  $10^{-15}$  (with `BLAST` hits otherwise set to default settings), followed by manual pruning of `BLAST` hits to remove hits not associated with functional genes. Since initial tests of these parameter settings suggested very few loci with functional gene `BLAST` hits (10%), we opted not to use more stringent filtering settings. We then used the Database for Annotation, Visualization, and Integrated Discovery (DAVID) to group gene hits by potential functional role (Dennis et al., 2003).

### 2.3 | Population differentiation

For each data set (neutral and outlier), we calculated population genetic summary statistics ( $H_O$ ,  $H_E$ , and  $F_{IS}$ ) using the function `gl.basic.stats` in packages `DARTR` and `ADEGENET` (Gruber et al., 2018; Jombart & Ahmed, 2011). For initial calculation of these summary statistics, we considered each sampling locality to be a separate population. We also calculated Watterson's theta ( $\theta_W$ ) and allelic richness ( $A$ ) using `ARLEQUIN` v.3.5.2.2 (Excoffier & Lischer, 2010). We calculated pairwise  $F_{ST}$  among focal regions, among sampling localities within focal regions, and among all sampling localities for both neutral and outlier data sets using packages `HIERFSTAT` and `DARTR` (Goudet, 2005). For pairwise  $F_{ST}$  calculations, we assessed significance by using 100 bootstrapped runs to assess significance and calculate 95% confidence intervals. We used Mantel correlation tests of Nei's  $D$  and geographic distance between individuals within each region and sampling locality to test for isolation-by-distance.

We then identified spatial clusters in neutral genetic variation using `TESS3R`, a spatially-explicit clustering approach. This approach calculates ancestry coefficients using a graph-based non-negative matrix factorization algorithm and uses information on spatial sample coordinates to control for population structure. We ran this model for  $K = 1$  to 8 using the projected least squares algorithm, visualized cross-validation scores for each value of  $K$ , and inferred the optimal  $K$  based on when cross-validation scores plateau or start increasing (Caye et al., 2016). As a point of comparison, we also identified clusters using `fastSTRUCTURE`, a nonspatial Bayesian approach to clustering (Raj et al., 2014). We ran the algorithm for  $K = 1$  to 8, and used the function “chooseK” to select the optimal value of  $K$  from these runs. Given low numbers of expected outlier loci, we did not explore clusters for the outlier data set.

### 2.4 | Simulations of demographic history

We employed two demographic analyses based on the folded site-frequency spectrum (SFS) to estimate changes in population sizes,

divergence dates, and gene flow. First, we estimated changes in effective population size over the past 100,000 years using the model-free, multiepoch coalescent method implemented in STAIRWAYPLOT v.2 (Liu & Fu, 2015). STAIRWAYPLOT uses the SFS and a mutation rate estimate as input, and its model-free estimation has been shown to outperform pairwise sequentially Markovian coalescent approaches (PSMC) for recent demographic histories (Li & Durbin, 2011). Second, we tested a suite of demographic scenarios based on different patterns of divergence, population size change, and gene flow using the model-based likelihood method implemented in FAST-SIMCOAL 2.6 (Excoffier et al., 2013). Briefly, this program generates expected SFS under user-specified demographic scenarios, which are then compared to the SFS generated from observed data (Excoffier et al., 2013; Rödin-Mörch et al., 2019). First, we imputed our neutral data set using the same approach outlined for outlier detection analyses to reduce issues with uneven proportions of missing data across sampling regions. Assuming four sampling regions (Austin, Elko, Hart, and Mono), we then used easySFS (<https://github.com/isaacovercast/easySFS>) to generate the SFS, projecting our neutral data set down to 30 individuals within each sampling region to produce between 14,677 (Mono) and 19,719 segregating sites (Austin), with counts of monomorphic sites approximated based on the total invariant base-pairs sequenced across all loci. While initial clustering analyses suggested support for within-region differentiation, we chose to focus on these four sampling regions for several reasons: (i)  $K = 4$  for fastSTRUCTURE supports broad-scale clustering between regions (Figure 2a), (ii) these four regions corresponded to the distribution of sampling effort in space, and thus represent a priori expectations for spatial genetic patterns, and (iii) a separate analysis of pairwise  $F_{ST}$  between sampling localities within and among regions indicated lower average  $F_{ST}$  between localities within the same region (average  $F_{ST} = 0.042$ ) relative to localities not in the same region (average  $F_{ST} = 0.094$ ; Supporting Information S3).

For model selection, we ran 50 replicates of each model with 400,000 simulations per replicate and estimated maximum-likelihood parameter values with the number of expectation conditional maximization cycles set to 40. We generated confidence intervals and ranges of parameter values by subsampling 70% of loci 25 times and running these 25 subsampled SFS 50 times each. Our alternative models were based on different hypothesized topologies for the history of regional divergence in the study area, as informed by two sources of information: (i) hierarchical structuring observed in initial analyses of genetic clustering, and (ii) previously studied Holocene and late Pleistocene biogeographic changes that have impacted the distribution of sagebrush (Byer et al., 2021; Figure 1). Briefly, this prior work leveraged a microsatellite data set to evaluate explanatory power of resistance surfaces that represent mid-Holocene and late-Pleistocene sagebrush cover (as proxies for interglacial and glacial periods, respectively; Byer et al., 2021; Millar & Woolfenden, 2016). The east-west model proposes that contemporary declines in sagebrush distribution in central Nevada have led to divergence between eastern and western regions, separating Mono and Hart from Elko and Austin (Figure 1b). The north-south model proposes

that the distribution of pluvial lakes near the last glacial maximum (22,000 years before present [YBP]) led to early divergence of regions to the north and south, splitting Mono and Austin from Elko and Hart (Figure 1c); this model mirrors initial clustering results at  $K = 2$ , which suggest broad-scale divergence between Austin and more northern regions (Elko and Hart-Sheldon; Figure 2a). Finally, we tested a model of early divergence between Mono and the other three regions, based on previous analyses showing differentiation of the Mono region (Larrucea et al., 2018) and initial clustering results that point to a distinct genetic cluster for Mono Basin from  $K = 4$  to  $K = 7$  (Figure 2a).

All models included estimates of historical gene flow in both directions between the ancestral populations, as well as contemporary migration between spatially proximate regions. Finally, since STAIRWAYPLOT results showed evidence of continuous bouts of population size change over long periods (see below), we used continuous growth rate parameters along each branch, based on the expected growth rate required to produce the sampled ancestral population sizes from current population sizes. During simulations, we used the mutation rate estimate for the mouse of  $5.7 \times 10^{-9}$ /bp/generation (Milholland et al., 2017). Effective population size was drawn from a uniform distribution of between 10 and either 5000, 50,000, or 200,000 individuals for current, recent ancestral, and the deepest ancestral lineages, respectively. Generation time for *B. idahoensis* is ~1 year (Stearns, 1992; Zeoli et al., 2008). We drew divergence times from a uniform distribution of between 100 and 15,000 generations (= years) for the most recent divergences in the models, and between 1000 and 150,000 generations for the ancestral divergence. Finally, the numbers of migrants per generation for each migration route specified in the model were drawn from a log-uniform distribution of between 0.00001 and 10 haploid individuals per generation, and converted to migration rates using the effective population size estimates (See Supporting Information S4 for the.est and.tpl files used to specify each model).

## 3 | RESULTS

### 3.1 | Outliers

In our PCADAPT analysis, we obtained principal components that separated individuals by study region (Supporting Information S5). The first principal component explained approximately 3% of variance, while the second through fifth components explained between 1.5% to 2% of variance each, followed by a plateau in cumulative percent of variance explained. We therefore chose the first five principal components for outlier detection. Ultimately, we detected 106 outliers out of 21,379 SNPs (0.5%) using a FDR of 0.05 for  $q$ -values. As in Luu et al. (2017), distributions of  $p$ -values visually adhered to a peak near zero and a uniform distribution of remaining  $p$ -values (Supporting Information S6).

We retained two environmental principal components for our investigation of GEAs using LFMM. The first principal component

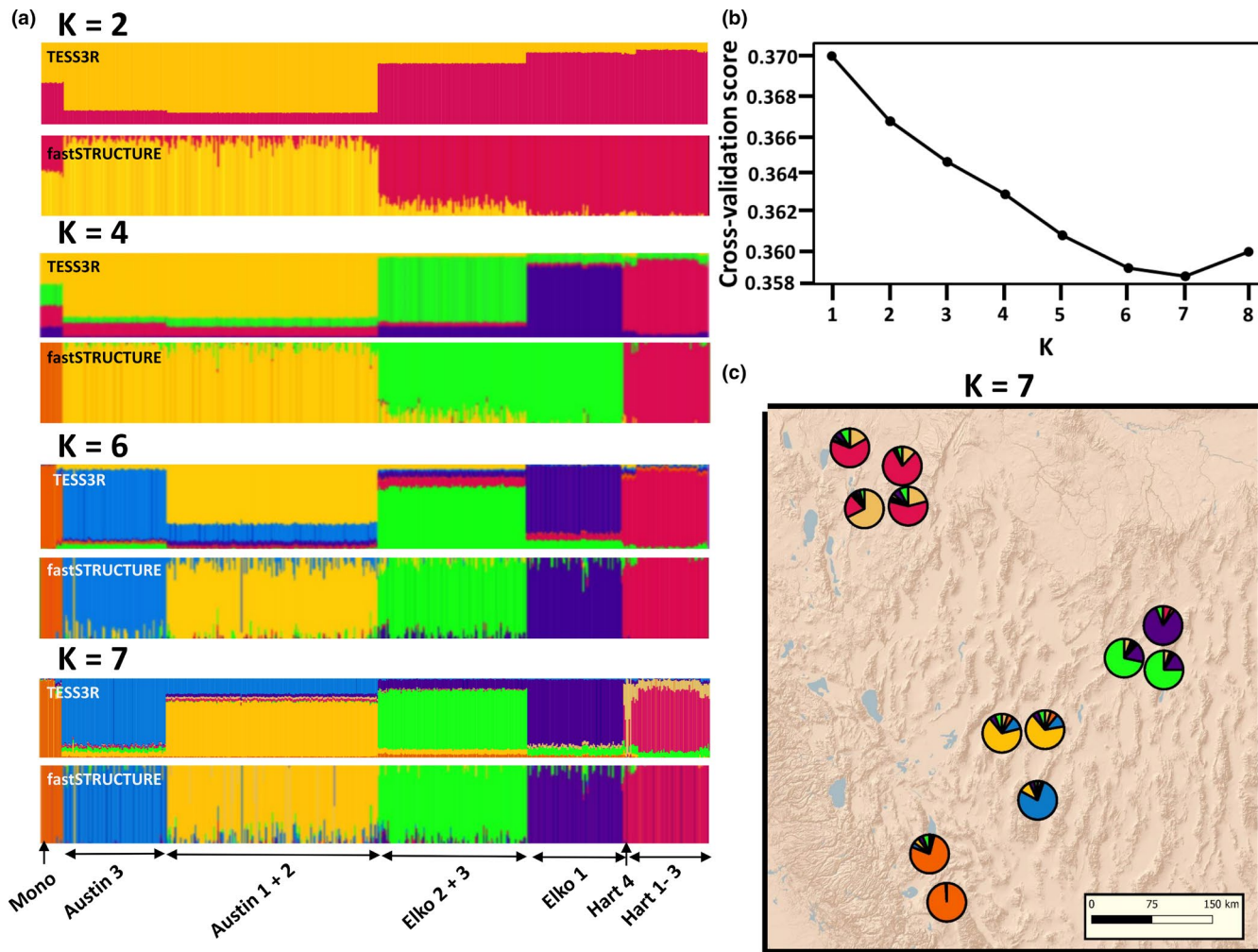


**FIGURE 2** Genetic structure of pygmy rabbit populations across the southern Great Basin. (a) Individual-level admixture proportions from  $K = 2, 4, 6$ , and  $7$  for fastSTRUCTURE and TESS3R. (b) Cross-validation plot for  $K = 1$  to  $8$  for TESS3R, indicating an elbow in cross-validation scores around  $K = 7$ . (c) Spatial clustering using the  $K = 7$  solution using TESS3R; each symbol designates population-level admixture proportions [Colour figure can be viewed at [wileyonlinelibrary.com](http://wileyonlinelibrary.com)]

highlighted gradients associated with mean annual temperatures, distance to intermittent and perennial streams, and precipitation in the coldest quarter, whereas the second highlighted associations between solar radiation, sandiness, sagebrush cover, and temperature seasonality. Inspection of sample sites within multivariate environmental space suggested slight separation between sample sites in the Mono Basin relative to sample sites in other study regions, although most sample sites grouped in a single environmental cluster near the origin (Supporting Information S7). Genomic inflation factors were very high for associations with both principal components ( $\lambda_1 = 5.96$ ,  $\lambda_2 = 7.83$ ) indicating extensive population structure in our data set (Rödin-Mörch et al., 2019). After correcting  $p$ -values based on these GIFs, we detected 46 outliers associated with PC1 (mean annual temperature and distance to intermittent/perennial streams) and 28 associated with PC2 (solar radiation, sandiness, and sage cover). Of these 74 SNPs, only four overlapped with the outliers detected using PCADAPT.

Our final outlier detection procedure used pRDA, with environmental variables conditioned on geographic location. The first

three constrained axes (RDA1, RDA2, and RDA3) explained 27.8%, 22.0%, and 21.7% of explainable variation after accounting for geographic effects, and were the only significant axes ( $p < .05$ ). Furthermore, although approximately 38% of explainable variation was multicollinear between geography and environment, approximately 62% was explained by environmental variables alone (Supporting Information S8). Given that these three axes collectively accounted for 72% of explainable variation, we restricted our remaining analyses to these three axes alone. Loci outside of the mean loading  $\pm 3$  SD on each axis were identified as outliers, which indicated 82 loci on RDA1, 45 on RDA2, and 61 on RDA3 as outlier loci, for a total of 188. Of these 188, eight overlapped with those found using LFMM and 51 overlapped with those found using PCADAPT. Although not a focus of analysis, excluding Mono Basin from outlier detection led to detection of nine, four, and 79 outliers from PCADAPT, LFMM, and pRDA, respectively, suggesting that many outliers originally detected for the Great Basin overall were associated with differentiation of the Mono Basin (Supporting Information S9).

Out of the 308 loci detected overall, 57 matched with existing genetic records using BLASTN (E-scores  $<1e-15$ ). We reduced these 57 matches down to 38 genes in the NCBI Gene database. Although we did not detect clustering in DAVID terms at an EASE score threshold of 0.05, we did detect significant enrichment (based on EASE score threshold of 0.05) in metal ion-binding genes (Supporting Information S10). We also investigated loci identified through each outlier detection method separately; using similar BLAST settings, 26 out of the 106 PCADAPT loci (24.5%), 14 out of 74 LFMM loci (16.7%), and 30 out of 188 pRDA loci (14.9%) matched to existing accessions, which were then reduced down to 24, 14, and 19 unique genes, respectively (Supporting Information S9). Genes identified in the PCADAPT data set included aldo-keto reductase family 1 member B, REC114 meiotic recombination protein, and FAT atypical cadherin 4 (Supporting Information S10). Genes identified in the LFMM data set included ADAM metallopeptidase 10, a heat shock protein 90 alpha family member, immunoglobulin kappa constant 1, a serine/threonine-protein kinase MARK2-like region, a microtubule interacting and trafficking domain, pericentrin, and a V-set and immunoglobulin domain-containing protein (Supporting Information S10). Genes identified within the pRDA data set included ATPase H<sup>+</sup>/K<sup>+</sup> transporting nongastric alpha2 subunit, a hypoxanthine phosphoribosyltransferase 1, a zinc finger protein 35, and G protein-coupled receptor 176 (Supporting Information S10). Only one outlier locus identified by all three methods was matched with a gene region of known function; this locus was matched to Sec23 homologue B (Supporting Information S10).

### 3.2 | Multivariate genotype-environment associations

Although the pRDA conducted for the overall SNP data set was primarily used to identify outlier loci, visualization of this constrained

ordination for the neutral data set revealed several features associated with genetic differentiation between study regions; we present this information to contextualize environmental gradients associated with genetic variation in pygmy rabbits (Figure 3). For the neutral data set, the first axis (RDA1) contrasted precipitation in the coldest month ( $r = -.87$ ) with distance to perennial and intermittent streams ( $r = .81$ ), temperature seasonality ( $r = .61$ ) and compound topographic index ( $r = .69$ ), the second (RDA2) captured variation in sage cover ( $r = .49$ ), precipitation in the coldest quarter ( $r = .38$ ), and soil sandiness ( $r = .35$ ), and the third (RDA3) contrasted precipitation in the warmest month ( $r = .76$ ) and sage cover ( $r = .52$ ) with temperature seasonality ( $r = -.70$ ) and mean annual temperature ( $r = -.58$ ). Furthermore, this pRDA captured spatial clustering in genetic variation as well (Figure 3a). Ordinations for the outlier data set highlighted similar environmental gradients to the neutral pRDA; unlike the neutral pRDA, only Mono Basin appeared to be differentiated along RDA1 (Figure 3b). Furthermore, Mono Basin was also related to RDA2 in contrasting directions between the neutral and outlier data sets (Figure 3b). In a similar fashion, the pRDA based on PCADAPT and LFMM outliers appeared to only highlight divergence in environmental and genetic space between Mono Basin and remaining Great Basin study regions (Supporting Information S11).

### 3.3 | Genetic differentiation and demographic history

After excluding the 308 outlier SNPs documented previously, our data set was comprised of 21,071 putatively neutral SNPs. The Mono Basin was the most genetically distinct region based on both the neutral (range of pairwise  $F_{ST}$  between other regions and Mono Basin = 0.099 to 0.133) and outlier data sets ( $F_{ST} = 0.375$  to 0.403; Table 1). Genetic distances within each region conformed to

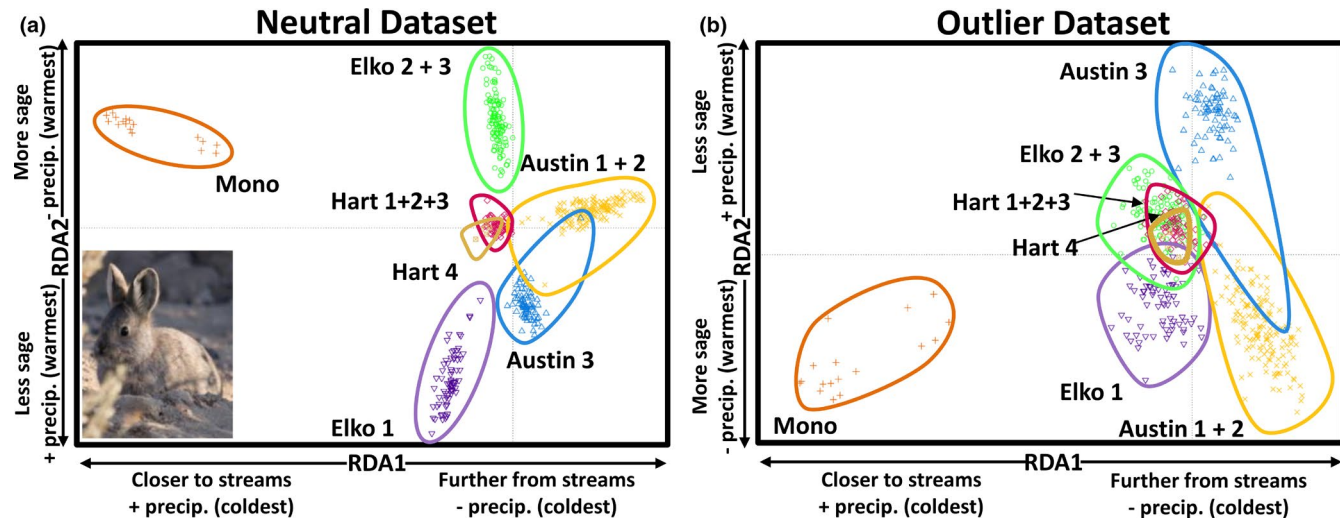


**FIGURE 3** Association of genetic and environmental variation as identified through partial redundancy analysis. Position of each cluster (as indicated by colours and ellipses) identified using TESS3R along redundancy axes (RDA1 and RDA2) for (a) the neutral data set and (b) the outlier data set. Primary variable loadings are described along each axis direction, and were generally similar between ordinations (although note opposite directions of associations along RDA2 between data sets) [Colour figure can be viewed at [wileyonlinelibrary.com](http://wileyonlinelibrary.com)]

isolation-by-distance for both neutral and outlier data sets (Table 2). Within regions, pairwise  $F_{ST}$  comparisons revealed some sampling localities that were more strongly differentiated than others, with consistent trends in neutral and outlier data sets. Within Austin, Austin 3 was strongly differentiated from other sampling localities (Table 3). Within Elko, Elko 1 appeared to be more strongly differentiated from other localities (Table 3, Figure 2c). Within Hart-Sheldon, Hart 4 appeared to be more strongly differentiated from other localities (Table 3). Every pairwise  $F_{ST}$  comparison between localities across all regions was significant for both neutral and outlier data sets (Table 3). Clustering using *tess3r* indicated strongest support for  $K = 7$  for the neutral data set, and revealed several key trends (Figure 2a,b). First, as suggested by regional analyses of genetic differentiation, sites in the Mono Basin were the most genetically differentiated. Second, sites in Elko formed two distinct clusters—one that included only Elko 1 and one that included only Elko 2 and 3. Third, Austin 3 appeared to be genetically distinct from nearly every site sampled. Finally, Hart 4 was assigned a unique cluster as well (Figure 2c). Clustering using *fastSTRUCTURE* indicated that  $K = 6$  maximized marginal likelihood; patterns of admixture for  $K = 6$  were relatively similar between clustering approaches (Figure 2a).

Model testing in *FASTSIMCOAL* showed that the Mono-early model was best supported (Figure 4a, Table 4a; full ranges of parameter values across bootstrapped runs presented below and in Table 4b). The Mono-early model received essentially all of the model weight ( $AIC = 442,442$ ,  $\omega = \sim 1$ ), while poor support existed for the east-west ( $AIC = 443,966$ ,  $\omega = \sim 0$ ) and north-south ( $AIC = 442,870$ ,  $\omega = \sim 0$ ). The best-supported model indicated a relatively ancient divergence between Mono and other regions, sometime between 62,000–214,000 YBP, with a more contemporary split between Hart, Elko, and Austin dating to 148–638 YBP (Figure 4a). Coalescent effective population sizes for each region were generally small, with lowest sizes for Mono (45–721) and Elko (5–290), and highest for Hart (208–1918) and Austin (185–1592). Stairway plots for each region corroborated the small contemporary effective population sizes and indicated magnitudes of population size change consistent with those recovered from *FASTSIMCOAL*. There were peaks in effective population size between 25,000 to 100,000 YBP for each region, with declines from 25,000 YBP to present (Figure 4b). Estimates for migration rates were highest from Elko to Austin (median = 6.31), from Elko to Hart (median = 2.67), from Hart to Elko (median = 2.55), and from Mono to Hart (median = 2.54; Table 4b).

## 4 | DISCUSSION

Species that are obligately linked to another should exhibit patterns of neutral and adaptive divergence driven by the taxon on which they are dependent (Gandon et al., 2008; Kaltz & Shykoff, 1998; Lively & Dybdahl, 2000). Pygmy rabbits are ecologically reliant on sagebrush, and our examination of both neutral and putatively adaptive genetic variation suggests that this dependence has had a substantive impact on the biogeography and molecular evolution of

the pygmy rabbit. We evaluated alternative models of demographic history across the southern Great Basin, and related genetic variation in neutral and outlier loci to current environmental gradients using multivariate approaches. Our major findings were: (i) the Mono Basin of California diverged and has been largely genetically isolated from the remainder of the range since the late Pleistocene, (b) despite having maintained low effective population sizes since the late Pleistocene, the Mono Basin region appears to be differentiated from the rest of the southern Great Basin at both neutral and outlier loci, (c) signatures of putative local adaptation across the southern Great Basin appear to be partly driven by availability of sagebrush, and (d) putatively adaptive loci were disproportionately common in gene regions associated with metal ion-binding; proteins that are involved in multiple metabolic pathways including binding of toxic compounds. Together, these data support the ecological and evolutionary influence that sagebrush availability and use has had on the pygmy rabbit.

### 4.1 | Demographic history

Our simulations of demographic history suggest that the Mono Basin diverged from the remainder of the range during climatic oscillations of the late Pleistocene (as a proxy for glacial conditions; Millar & Woolfenden, 2016). Reconstruction of historic sagebrush distribution suggests that both interglacial and glacial distributions were limited between the Mono Basin and the remainder of the Great Basin. Albeit largely isolated, Mono Basin connections to the populations immediately to the east (Austin region) may have been more probable during interglacial periods, while connections to the northern regions (Hart) may have been more common during interglacial periods (Figure 1). The latter scenarios are supported by gene flow parameter estimates showing genetic connectivity, albeit limited, between Hart and Mono is higher and thus perhaps more recent, than between Austin and Mono. Although no pygmy rabbit populations are known to be currently extant between Mono Basin and northwestern Nevada, museum records do exist from 1926 in Lassen County (U.C. Berkeley Accession MVM:Mamm: 36346–36362, 36368, 36369, 39870), suggesting that pygmy rabbits were probably more abundant between Mono and Hart during the recent past.

Our estimates of effective size through time (Figure 4b) show concerted, precipitous declines across the southern range initiating between 5000 and 10,000 YBP that have continued to today. This is consistent with the decline of pygmy rabbits in the fossil record beginning in the mid-Holocene, which also coincides with decline of sagebrush in the paleorecord (Commendador & Finney, 2016; Grayson, 2006). The southern (Austin) and eastern (Elko) portions of the range may have begun to decline during the end of the Pleistocene (Figure 4b). Albeit in decline, sagebrush distribution may have allowed limited gene flow among pygmy rabbit populations of the Austin, Elko and Hart regions until the past several hundred years, which is consistent with the lack of genetic structure in

**TABLE 1** Pairwise  $F_{ST}$  among study regions for (a) the neutral data set and (b) the outlier data set.  $F_{ST}$  values are shown below the diagonal and permutation-based 95% confidence intervals are shown above the diagonal

|              | Austin | Elko        | Hart-Sheldon | Mono Basin  |
|--------------|--------|-------------|--------------|-------------|
| (a)          |        |             |              |             |
| Austin       |        | 0.030–0.031 | 0.054–0.056  | 0.096–0.100 |
| Elko         | 0.030  |             | 0.044–0.046  | 0.100–0.104 |
| Hart-Sheldon | 0.055  | 0.045       |              | 0.128–0.133 |
| Mono Basin   | 0.098  | 0.102       | 0.130        |             |
| (b)          |        |             |              |             |
| Austin       |        | 0.059–0.080 | 0.062–0.090  | 0.372–0.435 |
| Elko         | 0.071  |             | 0.060–0.089  | 0.342–0.401 |
| Hart-Sheldon | 0.077  | 0.074       |              | 0.353–0.410 |
| Mono Basin   | 0.403  | 0.375       | 0.378        |             |

previous genetic data sets across this region (Larrucea et al., 2018). Finally, the Elko region is central to the overall range of the pygmy rabbit and appears to have been an important source of gene flow into other regions, but the cause of apparent recent precipitous declines in effective size warrant further investigation.

#### 4.2 | Environmental associations and signatures of local adaptation

By coupling detailed demographic analysis with information on environmental correlates of putative adaptive differentiation, we are able to make an initial hypothesis of the relative influences of drift and natural selection on genetic differentiation in the southern Great Basin. Although signatures of putative adaptive divergence were evident across all focal regions in our study, pairwise  $F_{ST}$  for our outlier data set was much higher for comparisons between Mono Basin and other regions, suggesting either (i) particularly strong signatures of local adaptation are present in this area, or (ii) spatial genetic structure from neutral processes may still be present in the outlier data set. Genetic differentiation in the Mono Basin samples also appeared to be strongly associated with RDA1, which contrasted precipitation in the coldest quarter with distance to streams and temperature indices. In contrast, RDA2, which contrasted sagebrush cover and precipitation in the warmest quarter, grouped Mono Basin samples differently between outlier and neutral data sets, potentially illustrating contrasting environmental relationships between the neutral and outlier data sets (Figure 3b). This suggests that the Mono Basin is environmentally unique, which may require unique adaptive responses for population persistence. These signatures of putative adaptive divergence appear to have emerged despite reductions in gene flow and effective population size through time.

Although associations between environmental and genetic differentiation were overall weaker for Austin, Elko, and Hart than for Mono, we documented two genetic clusters not discovered by Larrucea et al. (2018): one that consisted solely of Austin 3, and the other that consisted of Elko 1. Austin 3 is surrounded by the Shoshone and Toiyabe mountain ranges and may be largely disconnected from remaining Austin populations and potentially exposed

to different climatic conditions relative to remaining sites, particularly increased snowfall. Finally, Elko 1 differentiated from remaining populations in Elko along axis RDA2 and was associated more strongly with lower sagebrush cover relative to other populations within Elko, suggesting the potential that sagebrush cover may be exerting selective pressure on these populations (Gabler et al., 2001; Katzner & Parker, 1997; Larrucea & Brussard, 2008; White et al., 1982).

#### 4.3 | Loci under putative divergent selection

Across all three of our screening methods, we identified a relatively small proportion of our overall data set (~1.7%) as outliers. This proportion is similar to those in other studies; for example Xuereb et al. (2018) identified 71 out of 3699 SNPs (~2%) as outliers using BayeScan and RDAs for the giant sea cucumber (*Parastichopus californicus*), Araneda et al. (2016) identified 58 out of 1240 SNPs (~5%) as outlier using LOSITAN for the Chilean blue mussel (*Mytilus chilensis*), and Rödin-Mörch et al. (2019) identified 812 out of 27,590 SNPs (~3%) as outliers using PCADAPT and LFMM for the moor frog (*Rana arvalis*). In addition, very few of our identified outliers overlapped between approaches, probably because each method varies in its consideration of environmental gradients (from no consideration for PCADAPT to PC-based representation for LFMM and pRDA) and represents population structure in a variety of ways (PCA-based for PCADAPT, latent factors for LFMM, constrained axes for pRDA). As in other studies, relatively few of our outlier loci (57 out of 308, or 18.5%, representing 38 unique gene IDs) matched to genes of known function, emphasizing a challenge of using reduced-representation approaches that target random parts of the genome when studying non-model organisms. Below, we highlight several notable functional categories among these genes.

The only significant enrichment detected was for metal ion-binding genes. This and other observed gene ontology terms in our outlier data set ("metal ion-binding", "zinc", "oxidoreductase") have all been previously associated with detoxification in a number of taxa, including bivalves (Cross et al., 2018; Silliman, 2019), plants (Gardiner et al., 2018; Silva-Brandão et al., 2017), and birds (Zimmerman et al.,

TABLE 2 Summary statistics for genetic diversity within each region for (a) the neutral data set and (b) the outlier data set

| Region       | n   | A    | $\theta_w$ | $H_o$ | $H_e$ | $F_{IS}$ | IBD                         |
|--------------|-----|------|------------|-------|-------|----------|-----------------------------|
| (a)          |     |      |            |       |       |          |                             |
| Austin       | 237 | 2.00 | 3120.06    | 0.27  | 0.27  | 0.006    | Yes ( $r = .45, p = .001$ ) |
| Austin 1     | 9   | 1.83 | 5110.84    | 0.27  | 0.27  | -0.005   | No ( $r = .22, p = .083$ )  |
| Austin 2     | 150 | 2.00 | 3339.69    | 0.27  | 0.28  | 0.013    | Yes ( $r = .06, p = .003$ ) |
| Austin 3     | 78  | 1.97 | 3640.20    | 0.26  | 0.27  | 0.013    | Yes ( $r = .09, p = .005$ ) |
| Elko         | 184 | 2.00 | 3236.00    | 0.26  | 0.27  | 0.034    | Yes ( $r = .60, p = .001$ ) |
| Elko 1       | 72  | 1.96 | 3638.64    | 0.26  | 0.26  | 0.016    | Yes ( $r = .05, p = .024$ ) |
| Elko 2       | 105 | 1.99 | 3518.78    | 0.26  | 0.27  | 0.028    | Yes ( $r = .09, p = .003$ ) |
| Elko 3       | 7   | 1.81 | 5340.66    | 0.25  | 0.27  | 0.046    | No ( $r = -.13, p = .750$ ) |
| Hart-Sheldon | 65  | 1.95 | 3659.32    | 0.25  | 0.25  | 0.012    | Yes ( $r = .36, p = .001$ ) |
| Hart 1       | 8   | 1.72 | 4584.67    | 0.24  | 0.24  | -0.009   | No ( $r = -.03, p = .583$ ) |
| Hart 2       | 46  | 1.92 | 3820.51    | 0.25  | 0.26  | 0.025    | Yes ( $r = .10, p = .014$ ) |
| Hart 3       | 5   | 1.69 | 5129.08    | 0.25  | 0.26  | 0.013    | No ( $r = -.21, p = .811$ ) |
| Hart 4       | 6   | 1.67 | 4699.20    | 0.24  | 0.24  | -0.012   | No ( $r = -.19, p = .800$ ) |
| Mono Basin   | 17  | 1.71 | 3637.74    | 0.21  | 0.21  | 0.012    | Yes ( $r = .85, p = .001$ ) |
| Mono 1       | 5   | 1.56 | 4168.66    | 0.21  | 0.22  | 0.001    | No ( $r = -.20, p = .800$ ) |
| Mono 2       | 12  | 1.62 | 3482.32    | 0.21  | 0.21  | 0.001    | No ( $r = .11, p = .151$ )  |
| (b)          |     |      |            |       |       |          |                             |
| Austin       | 237 | 1.98 | 44.97      | 0.24  | 0.23  | -0.034   | Yes ( $r = .77, p = .001$ ) |
| Austin 1     | 9   | 1.74 | 66.29      | 0.24  | 0.22  | -0.063   | No ( $r = .12, p = .357$ )  |
| Austin 2     | 150 | 1.97 | 47.62      | 0.21  | 0.21  | -0.001   | No ( $r = .02, p = .254$ )  |
| Austin 3     | 78  | 1.93 | 50.68      | 0.26  | 0.26  | -0.014   | Yes ( $r = .15, p = .006$ ) |
| Elko         | 184 | 1.99 | 47.04      | 0.24  | 0.24  | -0.003   | Yes ( $r = .66, p = .001$ ) |
| Elko 1       | 72  | 1.91 | 50.51      | 0.24  | 0.24  | -0.016   | No ( $r = .04, p = .088$ )  |
| Elko 2       | 105 | 1.98 | 51.00      | 0.24  | 0.24  | 0.003    | No ( $r = .02, p = .348$ )  |
| Elko 3       | 7   | 1.74 | 72.01      | 0.25  | 0.25  | 0.000    | No ( $r = .17, p = .228$ )  |
| Hart-Sheldon | 65  | 1.91 | 51.28      | 0.24  | 0.23  | -0.037   | Yes ( $r = .36, p = .001$ ) |
| Hart 1       | 8   | 1.66 | 61.18      | 0.24  | 0.23  | -0.052   | No ( $r = .01, p = .492$ )  |
| Hart 2       | 46  | 1.86 | 52.22      | 0.25  | 0.24  | -0.012   | No ( $r = .04, p = .222$ )  |
| Hart 3       | 5   | 1.65 | 70.34      | 0.26  | 0.24  | -0.054   | No ( $r = -.46, p = .894$ ) |
| Hart 4       | 6   | 1.61 | 62.25      | 0.23  | 0.22  | -0.016   | No ( $r = -.13, p = .640$ ) |
| Mono Basin   | 17  | 1.77 | 57.96      | 0.27  | 0.28  | 0.020    | Yes ( $r = .86, p = .001$ ) |
| Mono 1       | 5   | 1.67 | 73.17      | 0.28  | 0.29  | 0.011    | No ( $r = -.05, p = .536$ ) |
| Mono 2       | 12  | 1.71 | 58.38      | 0.26  | 0.26  | -0.001   | No ( $r = -.01, p = .490$ ) |

Note: n, sample size; A, mean allelic richness;  $\theta_w$ , Watterson's estimator;  $H_o$ , observed heterozygosity;  $H_e$ , expected heterozygosity;  $F_{IS}$ , inbreeding coefficient. The IBD column indicates if significant isolation-by-distance was detected within the specified sampling region or locality.

2019). Most important, these genes are often enriched in adaptively divergent outlier data sets for taxa with dietary specialization. In the Gunnison's sage-grouse (*Centrocercus minimus*), Zimmerman et al. (2019) found significant enrichment in cytochrome P450 gene regions, which have functions associated with metabolism of PSCs through metal ion-binding and oxidoreductase activity. As with the pygmy rabbit, the Gunnison's sage-grouse is a sagebrush obligate, relying on sagebrush both for diet and shelter (Zimmerman et al., 2019). Since sagebrush species vary in composition and quantities

of PSCs, Zimmerman et al. (2019) suggested that variation in genes associated with metabolism of PSCs may reflect local adaptation to different species of sagebrush (Frye et al., 2013; Kelsey et al., 1982; Zimmerman et al., 2019). Pygmy rabbits are largely reliant on big sagebrush (*Artemisia tridentata*) and appear to be highly efficient at reducing concentrations of monoterpenes in their gut (Shipley et al., 2006; White et al., 1982); however, they often live in close proximity to other species of sagebrush such as the threetip sagebrush (*A. tripartita*) and may consume both when available (Green & Flinders,

**TABLE 3** Pairwise  $F_{ST}$  within sampling localities in each region.  $F_{ST}$  values for the neutral data set are shown below the diagonal and  $F_{ST}$  values for the outlier data set are shown above the diagonal

| Region = Austin       |          |          |          |        |
|-----------------------|----------|----------|----------|--------|
|                       | Austin 1 | Austin 2 | Austin 3 |        |
| Austin 1              | 0        | 0.020    | 0.090    |        |
| Austin 2              | 0.018    | 0        | 0.124    |        |
| Austin 3              | 0.041    | 0.030    | 0        |        |
| Region = Elko         |          |          |          |        |
|                       | Elko 1   | Elko 2   | Elko 3   |        |
| Elko 1                | 0        | 0.100    | 0.083    |        |
| Elko 2                | 0.039    | 0        | 0.005    |        |
| Elko 3                | 0.038    | 0.007    | 0        |        |
| Region = Hart-Sheldon |          |          |          |        |
|                       | Hart 1   | Hart 2   | Hart 3   | Hart 4 |
| Hart 1                | 0        | 0.041    | 0.053    | 0.079  |
| Hart 2                | 0.035    | 0        | 0.021    | 0.045  |
| Hart 3                | 0.047    | 0.021    | 0        | 0.041  |
| Hart 4                | 0.073    | 0.045    | 0.046    | 0      |
| Region = Mono Basin   |          |          |          |        |
|                       | Mono 1   | Mono 2   |          |        |
| Mono 1                | 0        | 0.101    |          |        |
| Mono 2                | 0.102    | 0        |          |        |

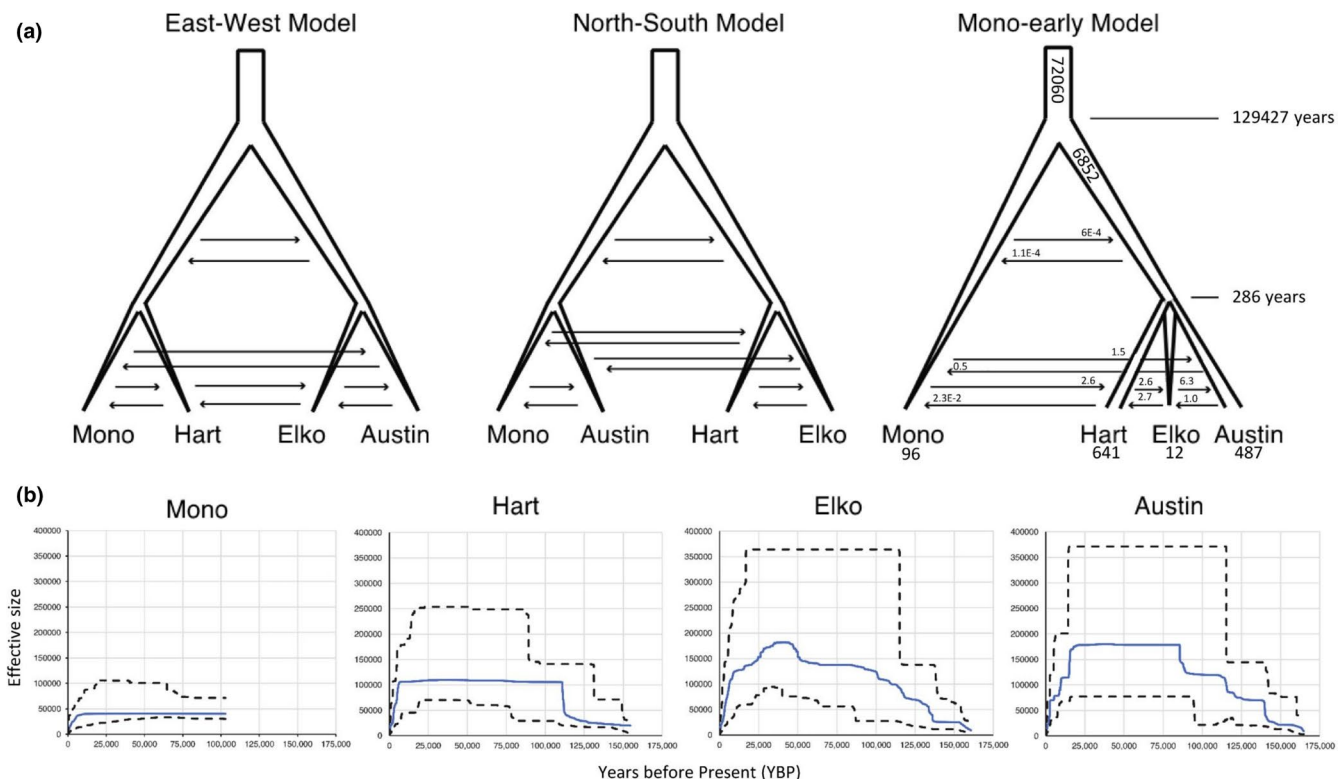


**FIGURE 4** Demographic history of pygmy rabbits across the southern Great Basin. (a) Alternative scenarios of divergence with gene flow and population size change in pygmy rabbits tested in FASTSIMCOAL 2.6. The Mono-early Model (third from left) was best supported by the coalescent simulations, and median estimates of parameter values across model runs on subsampled data sets are presented. Diploid sizes are presented for convenience. Arrows indicate directional migration (in effective migrants/generation) between focal regions. (b) Effective population size through time for each focal region showing concerted recent population declines across regions [Colour figure can be viewed at [wileyonlinelibrary.com](http://wileyonlinelibrary.com)]

**TABLE 4** (a) Relative rankings of demographic history models, as evaluated in FASTSIMCOAL. K = number of parameters, LL = log likelihood, AIC = Akaike's Information Criterion,  $\Delta$ AIC = change in AIC relative to the top model, and  $\omega$  = model selection weight. (b) Quartiles of divergence times (T), diploid effective population sizes (N), and diploid effective migration rates (MIG) for nonparametric bootstrapped runs, produced from 25 subsampled data sets each subjected to 50 replicate runs

| (a)  |         |              |             |              |           |
|--|---------|--------------|-------------|--------------|-----------|
| Model  | K       | LL           | AIC         | $\Delta$ AIC | $\omega$  |
| Mono-Early   | 18      | -96,067.166  | 442,441.649 | 0            | 1         |
| North-South  | 20      | -96,159.275  | 442,869.826 | 428.177621   | 1.053E-93 |
| East-West  | 20      | -96,397.265  | 443,965.811 | 1524.16207   | 0         |
| (b)  |         |              |             |              |           |
| Parameter  | Minimum | 25% Quartile | Median      | 75% Quartile | Maximum   |
| $N_{\text{Mono}}$  | 45      | 69           | 96          | 368          | 721       |
| $N_{\text{Hart}}$  | 208     | 438          | 641         | 985          | 1918      |
| $N_{\text{Elko}}$  | 5       | 9            | 12          | 30           | 290       |
| $N_{\text{Austin}}$  | 185     | 359          | 487         | 764          | 1592      |
| $N_{\text{Ancestral}}$   | 44,371  | 62,742       | 72,060      | 91,663       | 112,200   |
| $N_{\text{Austin/Elko/Hart}}$                                  | 709     | 1958         | 6852        | 17,080       | 28,100    |
| $T_{\text{Ancestral}}$   | 62,089  | 79,666       | 129,427     | 177,366      | 213,968   |
| $T_{\text{Austin/Elko/Hart}}$                                  | 148     | 230          | 286         | 489          | 638       |
| $\text{MIG}_{\text{Mono} \rightarrow \text{Austin/Elko/Hart}}$ | 1.51E-4 | 3.37E-4      | 6.26E-4     | 1.11E-3      | 0.22      |
| $\text{MIG}_{\text{Austin/Elko/Hart} \rightarrow \text{Mono}}$ | 5.53E-5 | 7.84E-5      | 1.09E-4     | 2.93E-4      | 6.01E-4   |
| $\text{MIG}_{\text{Mono} \rightarrow \text{Hart}}$             | 0.67    | 1.95         | 2.54        | 3.46         | 6.18      |
| $\text{MIG}_{\text{Hart} \rightarrow \text{Mono}}$             | 1.26E-4 | 2.08E-3      | 2.26E-2     | 0.26         | 0.58      |
| $\text{MIG}_{\text{Hart} \rightarrow \text{Elko}}$             | 8.1E-3  | 2.15         | 2.55        | 3.06         | 4.11      |
| $\text{MIG}_{\text{Elko} \rightarrow \text{Hart}}$             | 3.43E-4 | 4.14E-2      | 2.67        | 7.93         | 9.92      |
| $\text{MIG}_{\text{Elko} \rightarrow \text{Austin}}$           | 2.73E-4 | 4.05         | 6.31        | 7.04         | 8.95      |
| $\text{MIG}_{\text{Austin} \rightarrow \text{Elko}}$           | 2.19E-4 | 0.40         | 0.95        | 1.21         | 2.91      |
| $\text{MIG}_{\text{Austin} \rightarrow \text{Mono}}$           | 5.20E-2 | 0.41         | 0.45        | 0.70         | 0.86      |
| $\text{MIG}_{\text{Mono} \rightarrow \text{Austin}}$           | 8.21E-4 | 5.48E-2      | 1.43        | 2.07         | 4.59      |

1980). Furthermore, volatile oil content varies even within species of sagebrush as a function of soil characteristics, with documented relationships between oil content and magnesium and phosphorus content in soils for big sagebrush (Powell, 1970). We acknowledge that zinc finger proteins have diverse functions and may thus not be associated with detoxification loci. However, similarity between our results and those of Zimmerman et al. (2019) – and the fact that zinc finger proteins often flank CYP450 tandem arrays, which have documented importance for detoxification (M. Holding, personal observation) – may indicate local adaptation in a sagebrush specialist to variation in PSCs across the landscape.

#### 4.4 | Conclusions

Genetic isolation may either accelerate the selective effects of local environmental conditions (Räsänen & Hendry, 2008) or decrease adaptive potential by reducing effective population sizes (Sultan & Spencer, 2002; Tigano & Friesen, 2016). In our study, signatures of putative local adaptation among and within our focal study

regions suggest the possibility that selection has shaped variation between these regions (Fraser et al., 2011; Rellstab et al., 2017; Richardson et al., 2014). For the Mono Basin, long-term divergence from other southern Great Basin regions (Figure 4a), low rates of immigration from other regions (Figure 4a), and marked differentiation associated with environmental gradients (Figure 1b) suggest that historical isolation may have facilitated the accumulation of locally-adapted alleles (Haldane, 1930; Tigano & Friesen, 2016). However, recent declines in effective population size (Figure 4b) may increase the influence of genetic drift and reduce the ability of these populations to respond to selection in the future (Tigano & Friesen, 2016). For Austin, Elko, and Hart, high rates of gene flow (Figure 4a), low environmental differentiation between regions (Figure 2), and reduced counts of outliers for outlier scans excluding Mono Basin may point to more modest adaptive differentiation among these regions, and reduced effects of genetic drift due to greater genetic connectivity throughout these regions. Overall, our study suggests that the Mono Basin is evolutionarily highly distinct and harbors the strongest signals of adaptive divergence among sites.

Nevertheless, environmental associations with outlier SNPs were relatively weak, with environment only explaining approximately 5% of total variance in the SNP data set (Supporting Information S7). This fact – combined with noticeable clustering by study region within multivariate space, substantial geographic separation between study regions, and relatively high degrees of multicollinearity between geographic and environmental variables – generates difficulties in separating purely environmental effects on genetic variation from those explainable by distance alone (Gaggiotti et al., 2009; Kawecki & Ebert, 2004; Räsänen & Hendry, 2008; Stiebens et al., 2013). Although redundancy analyses are robust to moderate to relatively high degrees of population differentiation (Forester et al., 2018), it is not clear if these detected signatures of putative adaptive divergence are more reflective of environmental differences or geographic separation between study sites; both are often viewed as important processes facilitating local adaptation, and may both be influential in the pygmy rabbit system (Kawecki & Ebert, 2004; Räsänen & Hendry, 2008; Sork et al., 2010). Further study is needed to determine how the interaction between environment, geography, and demographic change through time affects genetic variation in this species.

#### 4.5 | Future directions

Although it remains to be seen if our observed outlier loci are (or are linked to) ecologically adaptive loci, differentially adapted populations may respond to environmental change in distinct ways, necessitating more dynamic and flexible conservation planning initiatives to account for these different responses (Hällfors et al., 2016; Hoffmann & Sgro, 2011). Efforts are underway to assemble a high-quality pygmy rabbit genome (Holding et al., 2021), and further work will leverage this genome to understand the genomic position of putatively adaptive SNPs. While our results mirror enrichment in detoxification loci documented in the Gunnison's sage-grouse (Zimmerman et al., 2019), we suspect that reappraisal of adaptive genetic variation with the aid of the pygmy rabbit genome may highlight even more gene families as potentially important for driving adaptive genetic divergence, particularly if SNPs not within functional gene regions are linked with detoxification loci (Lowry et al., 2017; although see Catchen et al., 2017). Since changes in genotype frequencies are mediated by selection on phenotypes, we suggest that future studies explore the relationships between phenotypes and fitness at both broad (between Mono Basin and remaining study regions) and finer (within Elko and Austin) scales. Furthermore, developing a better understanding of local adaptation will be important in predicting how populations will respond to ongoing environmental change (Hoffmann & Sgro, 2011; Schoville et al., 2011).

#### ACKNOWLEDGEMENTS

For assistance in the field we thank: S. Appleby, K. Durham, S. Heissenberger, D. Hulton, E. Hunter, C. Jones, E. Ketchian, J. Knapp, H. Ludwig, D. Miles, A. Mitchell, N. Murphy, S. Olson, H. Phares,

B. Rapier, K. Rich, S. Sandefur, L. Smith, C. Turner, K. Vanchena, J. VanGunst, and A. Van Geem. Many agency biologists gave us generous logistical assistance and access to land; for facilitating the initiation and conduct of this work we thank: K. Boatner, N. Burton, D. Catalano, G. Collins, S. Espinosa, M. Freese, K. Goldie, M. Jeffress, J. Kasbohm, R. Lamp, J. Newmark, D. Probasco, J. Tull, J. VanGunst, and M. West. We thank K. Graski, and J. Knapp for assistance in the lab, and T. Glenn for access to laboratory space. C. Feldman, M. Logan, J. Ouyang, and the UNR EvolDoers provided helpful comments on a previous version of this manuscript. We thank S. Zimmerman, T. Glenn, S. Lance, and J. Forbey for helpful discussions. This research was made possible by grants from U.S. Fish and Wildlife, Nevada Department of Wildlife, Greater Hart Sheldon Fund, the Great Basin Landscape Conservation Cooperative, and the National Science Foundation (OIA-1826801).

#### AUTHOR CONTRIBUTIONS

Nathan W. Byer wrote the manuscript with the help of Matthew L. Holding and Marjorie D. Matocq. Marjorie D. Matocq and Kevin T. Shoemaker obtained funding. Nathan W. Byer, Matthew L. Holding, and Todd W. Pierson performed bioinformatics and statistical analyses. Nathan W. Byer, Thomas E. Dilts, and Kevin T. Shoemaker acquired and processed environmental data for analysis. Todd W. Pierson performed the laboratory work. Miranda M. Crowel, Kevin T. Shoemaker, and Marjorie D. Matocq performed field surveys. All authors contributed to study design and conceptualization and contributed to the final version of the manuscript.

#### DATA AVAILABILITY STATEMENT

Illumina data are publicly available at NCBI (BioProject PRJNA732667) and filtered SNPs have been made available through Dryad (<https://doi.org/10.5061/dryad.6hdr7sr15>).

#### ORCID

Nathan W. Byer  <https://orcid.org/0000-0003-3230-7384>

#### REFERENCES

- Altschul, S. F., Gish, W., Miller, W., Myers, E. W., & Lipman, D. J. (1990). Basic local alignment search tool. *Journal of Molecular Biology*, 215(3), 403–410. [https://doi.org/10.1016/S0022-2836\(05\)80360-2](https://doi.org/10.1016/S0022-2836(05)80360-2)
- Araneda, C., Larrain, M. A., Hecht, B., & Narum, S. (2016). Adaptive genetic variation distinguishes Chilean blue mussels (*Mytilus chilensis*) from different marine environments. *Ecology and Evolution*, 6, 3632–3644. <https://doi.org/10.1002/ece3.2110>
- Bayona-Vásquez, N. J., Glenn, T. C., Kieran, T. J., Pierson, T. W., Hoffberg, S. L., Scott, P. A., Bentley, K. E., Finger, J. W., Louha, S., Troendle, N., Diaz-Jaimes, P., Mauricio, R., & Faircloth, B. C. (2019). Adapterama III: Quadruple-indexed, double/triple-enzyme RADseq libraries (2RAD/3RAD). *PeerJ*, 7, e7724. <https://doi.org/10.7717/peerj.7724>
- Byer, N. W., Dilts, T. E., Larrucea, E. S., Crowell, M. M., Shoemaker, K. T., Weisberg, P. J., & Matocq, M. D. (2021). Holocene-era landscape changes affect genetic connectivity in a sagebrush obligate species, the Pygmy Rabbit (*Brachylagus idahoensis*) (Manuscript submitted to *Landscape Ecology*).
- Capblancq, T., Luu, K., Blum, M. G., & Bazin, E. (2018). Evaluation of redundancy analysis to identify signatures of local adaptation.

Molecular Ecology Resources, 18(6), 1223–1233. <https://doi.org/10.1111/1755-0998.12906>

Catchen, J. M., Hohenlohe, P. A., Bernatchez, L., Funk, W. C., Andrews, K. R., & Allendorf, F. W. (2017). Unbroken: RADseq remains a powerful tool for understanding the genetics of adaptation in natural populations. *Molecular Ecology Resources*, 17(3), 362–365. <https://doi.org/10.1111/1755-0998.12669>

Caye, K., Deist, T. M., Martins, H., Michel, O., & François, O. (2016). TESS3: Fast inference of spatial population structure and genome scans for selection. *Molecular Ecology Resources*, 16(2), 540–548. <https://doi.org/10.1111/1755-0998.12471>

Commendador, A. S., & Finney, B. P. (2016). Holocene environmental change in the eastern Snake River Plain of Idaho, USA, as inferred from stable isotope analyses of small mammals. *Quaternary Research*, 85(3), 358–370. <https://doi.org/10.1016/j.yqres.2016.03.008>

Coulon, A., Cosson, J. F., Angibault, J. M., Cargnelutti, B., Galan, M., Morellet, N., Petit, E., Aulagnier, S., & Hewison, A. J. M. (2004). Landscape connectivity influences gene flow in a roe deer population inhabiting a fragmented landscape: An individual-based approach. *Molecular Ecology*, 13(9), 2841–2850. <https://doi.org/10.1111/j.1365-294X.2004.02253.x>

Crawford, J. A., Anthony, R. G., Forbes, J. T., & Lorton, G. A. (2010). Survival and causes of mortality for pygmy rabbits (*Brachylagus idahoensis*) in Oregon and Nevada. *Journal of Mammalogy*, 91(4), 838–847.

Cross, I., Portela-Bens, S., García-Angulo, A., Merlo, M. A., Rodríguez, M. E., Liehr, T., & Rebordinos, L. (2018). A preliminary integrated genetic map distinguishes every chromosome pair and locates essential genes related to abiotic adaptation of *Crassostrea angulata/gigas*. *BMC Genetics*, 19(1), 104. <https://doi.org/10.1186/s12863-018-0689-5>

Crowell, M., Shoemaker, K., & Matocq, M. (2020). Ideal conditions for increased trapping success of pygmy rabbits (*Brachylagus idahoensis*) across the Great Basin. *Journal of Mammalogy*, 101, 1736–1749.

Cushman, S. A., McKelvey, K. S., Hayden, J., & Schwartz, M. K. (2006). Gene flow in complex landscapes: Testing multiple hypotheses with causal modeling. *The American Naturalist*, 168, 486–499. <https://doi.org/10.1086/506976>

Dennis, G. Jr, Sherman, B. T., Hosack, D. A., Yang, J., Gao, W., Lane, H. C., & Lempicki, R. A. (2003). DAVID: Database for annotation, visualization, and integrated discovery. *Genome Biology*, 4(9), R60. <https://doi.org/10.1186/gb-2003-4-9-r60>

Dilts, T. E., & Shoemaker, K. T. (2020). Spatial layers for habitat modelling in the pygmy rabbit (*Brachylagus idahoensis*) (unpublished data).

Dixon, P. (2003). VEGAN, a package of R functions for community ecology. *Journal of Vegetation Science*, 14(6), 927–930. <https://doi.org/10.1111/j.1654-1103.2003.tb02228.x>

Dobler, F. C., & Dixon, K. R. (1990). The pygmy rabbit *Brachylagus idahoensis*. Rabbits, hares, and pikas: Status survey and conservation action plan (JA Chapman and JEC Flux, eds.). IUCN/SSC Lagomorph Specialist Group, Gland, Switzerland, 111–115.

Eaton, D. A., & Overcast, I. (2020). ipyrad: Interactive assembly and analysis of RADseq datasets. *Bioinformatics*, 36(8), 2592–2594. <https://doi.org/10.1093/bioinformatics/btz966>

Elias, B. A., Shipley, L. A., McCusker, S., Sayler, R. D., & Johnson, T. R. (2013). Effects of genetic management on reproduction, growth, and survival in captive endangered pygmy rabbits (*Brachylagus idahoensis*). *Journal of Mammalogy*, 94(6), 1282–1292.

Estes-Zumpf, W. A., Rachlow, J. L., Waits, L. P., & Warheit, K. I. (2010). Dispersal, gene flow, and population genetic structure in the pygmy rabbit (*Brachylagus idahoensis*). *Journal of Mammalogy*, 91(1), 208–219.

Excoffier, L., Dupanloup, I., Huerta-Sánchez, E., Sousa, V. C., & Foll, M. (2013). Robust demographic inference from genomic and SNP data. *PLoS Genetics*, 9(10), e1003905. <https://doi.org/10.1371/journal.pgen.1003905>

Excoffier, L., & Lischer, H. E. (2010). Arlequin suite ver 3.5: A new series of programs to perform population genetics analyses under Linux and Windows. *Molecular Ecology Resources*, 10(3), 564–567.

Fischer, M. C., Rellstab, C., Leuzinger, M., Roumet, M., Gugerli, F., Shimizu, K. K., Holderegger, R., & Widmer, A. (2017). Estimating genomic diversity and population differentiation – An empirical comparison of microsatellite and SNP variation in *Arabidopsis halleri*. *BMC Genomics*, 18(1), 69. <https://doi.org/10.1186/s12864-016-3459-7>

Fitzpatrick, M. C., & Keller, S. R. (2015). Ecological genomics meets community-level modelling of biodiversity: Mapping the genomic landscape of current and future environmental adaptation. *Ecology Letters*, 18(1), 1–16. <https://doi.org/10.1111/ele.12376>

Forester, B. R., Jones, M. R., Joost, S., Landguth, E. L., & Lasky, J. R. (2016). Detecting spatial genetic signatures of local adaptation in heterogeneous landscapes. *Molecular Ecology*, 25(1), 104–120. <https://doi.org/10.1111/mec.13476>

Forester, B. R., Lasky, J. R., Wagner, H. H., & Urban, D. L. (2018). Comparing methods for detecting multilocus adaptation with multivariate genotype–environment associations. *Molecular Ecology*, 27(9), 2215–2233. <https://doi.org/10.1111/mec.14584>

Fraser, D. J., Weir, L. K., Bernatchez, L., Hansen, M. M., & Taylor, E. B. (2011). Extent and scale of local adaptation in salmonid fishes: Review and meta-analysis. *Heredity*, 106(3), 404. <https://doi.org/10.1038/hdy.2010.167>

Frichot, E., & François, O. (2015). LEA: An R package for landscape and ecological association studies. *Methods in Ecology and Evolution*, 6(8), 925–929. <https://doi.org/10.1111/2041-210X.12382>

Frichot, E., Schoville, S. D., Bouchard, G., & François, O. (2013). Testing for associations between loci and environmental gradients using latent factor mixed models. *Molecular Biology and Evolution*, 30(7), 1687–1699. <https://doi.org/10.1093/molbev/mst063>

Frye, G. G., Connelly, J. W., Musil, D. D., & Forbey, J. S. (2013). Phytochemistry predicts habitat selection by an avian herbivore at multiple spatial scales. *Ecology*, 94(2), 308–314. <https://doi.org/10.1890/12-1313.1>

Gabler, K. I., Heady, L. T., & Laundré, J. W. (2001). A habitat suitability model for pygmy rabbits (*Brachylagus idahoensis*) in southeastern Idaho. *Western North American Naturalist*, 61, 480–489.

Gaggiotti, O. E., Bekkevold, D., Jørgensen, H. B., Foll, M., Carvalho, G. R., Andre, C., & Ruzzante, D. E. (2009). Disentangling the effects of evolutionary, demographic, and environmental factors influencing genetic structure of natural populations: Atlantic herring as a case study. *Evolution: International Journal of Organic Evolution*, 63(11), 2939–2951.

Gandon, S., Buckling, A., Demeure, E., & Day, T. (2008). Host–parasite coevolution and patterns of adaptation across time and space. *Journal of Evolutionary Biology*, 21(6), 1861–1866. <https://doi.org/10.1111/j.1420-9101.2008.01598.x>

Gardiner, L.-J., Joynson, R., Omony, J., Rusholme-Pilcher, R., Olohan, L., Lang, D., Bai, C., Hawkesford, M., Salt, D., Spannagl, M., Mayer, K. F. X., Kenny, J., Bevan, M., Hall, N., & Hall, A. (2018). Hidden variation in polyploid wheat drives local adaptation. *Genome Research*, 28(9), 1319–1332. <https://doi.org/10.1101/gr.233551.117>

Gibbs, J. P. (2001). Demography versus habitat fragmentation as determinants of genetic variation in wild populations. *Biological Conservation*, 100, 15–20. [https://doi.org/10.1016/S0006-3207\(00\)00203-2](https://doi.org/10.1016/S0006-3207(00)00203-2)

Goudet, J. (2005). Hierfstat, a package for R to compute and test hierarchical F-statistics. *Molecular Ecology Notes*, 5(1), 184–186. <https://doi.org/10.1111/j.1471-8286.2004.00828.x>

Grayson, D. K. (2006). The Late Quaternary biogeographic histories of some Great Basin mammals (western USA). *Quaternary Science Reviews*, 25(21–22), 2964–2991. <https://doi.org/10.1016/j.quascirev.2006.03.004>

Green, J. S., & Flinders, J. T. (1980). Habitat and dietary relationships of the pygmy rabbit. *Rangeland Ecology & Management/Journal*

of *Range Management Archives*, 33(2), 136–142. <https://doi.org/10.2307/3898429>

Gruber, B., Unmack, P. J., Berry, O. F., & Georges, A. (2018). dartr: An R package to facilitate analysis of SNP data generated from reduced representation genome sequencing. *Molecular Ecology Resources*, 18(3), 691–699.

Haldane, J. (1930). Theoretical genetics of autopolyploids. *Journal of Genetics*, 22(3), 359–372. <https://doi.org/10.1007/BF02984197>

Hällfors, M. H., Liao, J., Dzurisin, J., Grundel, R., Hyvärinen, M., Towle, K., Wu, G. C., & Hellmann, J. J. (2016). Addressing potential local adaptation in species distribution models: Implications for conservation under climate change. *Ecological Applications*, 26(4), 1154–1169. <https://doi.org/10.1890/15-0926>

Hanski, I., Mononen, T., & Ovaskainen, O. (2011). Eco-evolutionary metapopulation dynamics and the spatial scale of adaptation. *The American Naturalist*, 177(1), 29–43. <https://doi.org/10.1086/657625>

Hauser, L., Baird, M., Hilborn, R., Seeb, L. W., & Seeb, J. E. (2011). An empirical comparison of SNPs and microsatellites for parentage and kinship assignment in a wild sockeye salmon (*Oncorhynchus nerka*) population. *Molecular Ecology Resources*, 11, 150–161.

Heywood, J. S. (1991). Spatial analysis of genetic variation in plant populations. *Annual Review of Ecology and Systematics*, 22(1), 335–355. <https://doi.org/10.1146/annurev.es.22.110191.002003>

Hoffmann, A. A., & Sgro, C. M. (2011). Climate change and evolutionary adaptation. *Nature*, 470, 479–485. <https://doi.org/10.1038/nature09670>

Hoffmann, A. A., & Willi, Y. (2008). Detecting genetic responses to environmental change. *Nature Reviews Genetics*, 9(6), 421–432. <https://doi.org/10.1038/nrg2339>

Holderegger, R., Kamm, U., & Gugerli, F. (2006). Adaptive vs. neutral genetic diversity: Implications for landscape genetics. *Landscape Ecology*, 21(6), 797–807.

Holding, M. L. et al. (2021). High quality pygmy rabbit (*Brachylagus idahoensis*) genome (Manuscript in progress).

Jombart, T., & Ahmed, I. (2011). adegenet 1.3-1: New tools for the analysis of genome-wide SNP data. *Bioinformatics*, 27(21), 3070–3071.

Kaltz, O., & Shykoff, J. A. (1998). Local adaptation in host-parasite systems. *Heredity*, 81(4), 361–370. <https://doi.org/10.1046/j.1365-2540.1998.00435.x>

Katzner, T. E., & Parker, K. L. (1997). Vegetative characteristics and size of home ranges used by pygmy rabbits (*Brachylagus idahoensis*) during winter. *Journal of Mammalogy*, 78(4), 1063–1072. <https://doi.org/10.2307/1383049>

Kawecki, T. J., & Ebert, D. (2004). Conceptual issues in local adaptation. *Ecology Letters*, 7(12), 1225–1241. <https://doi.org/10.1111/j.1461-0248.2004.00684.x>

Kelsey, R. G., Stephens, J. R., & Shafizadeh, F. (1982). The chemical constituents of sagebrush foliage and their isolation. *Journal of Range Management*, 35(5), 617–622. <https://doi.org/10.2307/3898650>

Keyghobadi, N. (2007). The genetic implications of habitat fragmentation for animals. *Canadian Journal of Zoology*, 85(10), 1049–1064.

Kohn, M. H., Murphy, W. J., Ostrander, E. A., & Wayne, R. K. (2006). Genomics and conservation genetics. *Trends in Ecology & Evolution*, 21(11), 629–637. <https://doi.org/10.1016/j.tree.2006.08.001>

Larruea, E. S., & Brussard, P. F. (2008). Habitat selection and current distribution of the pygmy rabbit in Nevada and California, USA. *Journal of Mammalogy*, 89(3), 691–699. <https://doi.org/10.1644/07-MAMM-A-199R.1>

Larruea, E. S., Robinson, M. L., Rippert, J. S., & Matocq, M. D. (2018). Genetically distinct populations of the pygmy rabbit (*Brachylagus idahoensis*) in the Mono Basin of California. *Journal of Mammalogy*, 99(2), 408–415. <https://doi.org/10.1093/jmammal/gyx187>

Larsen, P. A., & Matocq, M. D. (2019). Emerging genomic applications in mammalian ecology, evolution, and conservation. *Journal of Mammalogy*, 100(3), 786–801. <https://doi.org/10.1093/jmammal/gyy184>

Li, H., & Durbin, R. (2011). Inference of human population history from individual whole-genome sequences. *Nature*, 475(7357), 493–496. <https://doi.org/10.1038/nature10231>

Liu, X., & Fu, Y.-X. (2015). Exploring population size changes using SNP frequency spectra. *Nature Genetics*, 47(5), 555–559. <https://doi.org/10.1038/ng.3254>

Lively, C. M., & Dybdahl, M. F. (2000). Parasite adaptation to locally common host genotypes. *Nature*, 405(6787), 679–681.

Loiselle, B. A., Sork, V. L., Nason, J., & Graham, C. (1995). Spatial genetic structure of a tropical understory shrub, *Psychotria officinalis* (Rubiaceae). *American Journal of Botany*, 82(11), 1420–1425.

Lowe, W. H., & Allendorf, F. W. (2010). What can genetics tell us about population connectivity? *Molecular Ecology*, 19, 3038–3051. <https://doi.org/10.1111/j.1365-294X.2010.04688.x>

Lowry, D. B., Hoban, S., Kelley, J. L., Lotterhos, K. E., Reed, L. K., Antolin, M. F., & Storfer, A. (2017). Breaking RAD: An evaluation of the utility of restriction site associated DNA sequencing for genome scans of adaptation. *Molecular Ecology Resources*, 17(2), 142–152. <https://doi.org/10.1111/1755-0998.12635>

Luu, K., Bazin, E., & Blum, M. G. (2017). pcadapt: An R package to perform genome scans for selection based on principal component analysis. *Molecular Ecology Resources*, 17(1), 67–77.

Mable, B. K. (2019). Conservation of adaptive potential and functional diversity: Integrating old and new approaches. *Conservation Genetics*, 20(1), 89–100. <https://doi.org/10.1007/s10592-018-1129-9>

Manel, S., Joost, S., Epperson, B. K., Holderegger, R., Storfer, A., Rosenberg, M. S., Scribner, K. T., Bonin, A., & Fortin, M.-J. (2010). Perspectives on the use of landscape genetics to detect genetic adaptive variation in the field. *Molecular Ecology*, 19(17), 3760–3772. <https://doi.org/10.1111/j.1365-294X.2010.04717.x>

Meyer-Lucht, Y., Mulder, K. P., James, M. C., McMahon, B. J., Buckley, K., Pierpoint, S. B., & Höglund, J. (2016). Adaptive and neutral genetic differentiation among Scottish and endangered Irish red grouse (*Lagopus lagopus scotica*). *Conservation Genetics*, 17(3), 615–630. <https://doi.org/10.1007/s10592-016-0810-0>

Milholland, B., Dong, X., Zhang, L., Hao, X., Suh, Y., & Vijg, J. (2017). Differences between germline and somatic mutation rates in humans and mice. *Nature Communications*, 8(1), 1–8. <https://doi.org/10.1038/ncomms15183>

Millar, C. I., & Woolfenden, W. B. (2016). Ecosystems past: Vegetation prehistory. In H. A. Mooney, & E. S. Zavaleta (Eds.), *Ecosystems of California: A comprehensive overview of the ecosystems of California, past, present and future* (pp. 131–186). University of California Press.

Powell, J. (1970). Site factor relationships with volatile oils in big sagebrush. *Rangeland Ecology & Management/Journal of Range Management Archives*, 23(1), 42–46. <https://doi.org/10.2307/3896006>

R Core Team (2020). *R: A language and environment for statistical computing*. R Foundation for Statistical Computing. Retrieved from <https://www.R-project.org/>

Raj, A., Stephens, M., & Pritchard, J. K. (2014). fastSTRUCTURE: Variational inference of population structure in large SNP data sets. *Genetics*, 197(2), 573–589. <https://doi.org/10.1534/genetics.114.164350>

Räsänen, K., & Hendry, A. P. (2008). Disentangling interactions between adaptive divergence and gene flow when ecology drives diversification. *Ecology Letters*, 11(6), 624–636. <https://doi.org/10.1111/j.1461-0248.2008.01176.x>

Rellstab, C., Fischer, M. C., Zoller, S., Graf, R., Tedder, A., Shimizu, K. K., Widmer, A., Holderegger, R., & Gugerli, F. (2017). Local adaptation (mostly) remains local: Reassessing environmental associations of climate-related candidate SNPs in *Arabidopsis halleri*. *Heredity*, 118(2), 193–201. <https://doi.org/10.1038/hdy.2016.82>

Richardson, J. L., Urban, M. C., Bolnick, D. I., & Skelly, D. K. (2014). Microgeographic adaptation and the spatial scale of evolution. *Trends in Ecology & Evolution*, 29(3), 165–176. <https://doi.org/10.1016/j.tree.2014.01.002>

Rödin-Mörch, P., Luquet, E., Meyer-Lucht, Y., Richter-Boix, A., Höglund, J., & Laurila, A. (2019). Latitudinal divergence in a widespread amphibian: Contrasting patterns of neutral and adaptive genomic variation. *Molecular Ecology*, 28(12), 2996–3011. <https://doi.org/10.1111/mec.15132>

Rousset, F. (2001). Inferences from spatial population genetics. In D. J. Balding, M. Bishop, & C. Cannings (Eds.), *Handbook of statistical genetics* (pp. 945–979). John Wiley & Sons, Ltd.

Savolainen, O., Lascoux, M., & Merilä, J. (2013). Ecological genomics of local adaptation. *Nature Reviews Genetics*, 14(11), 807. <https://doi.org/10.1038/nrg3522>

Schoville, S. D., Bonin, A., François, O., Lobreaux, S., Melodelima, C., & Manel, S. (2011). Adaptive genetic variation on the landscape: Methods and cases. *Annual Review of Ecology, Evolution, and Systematics*, 43(1), 23–43. <https://doi.org/10.1146/annurev-ecolsys-110411-160248>

Segelbacher, G., Cushman, S. A., Epperson, B. K., Fortin, M.-J., Francois, O., Hardy, O. J., Holderegger, R., Taberlet, P., Waits, L. P., & Manel, S. (2010). Applications of landscape genetics in conservation biology: Concepts and challenges. *Conservation Genetics*, 11, 375–385. <https://doi.org/10.1007/s10592-009-0044-5>

Shipley, L. A., Davila, T. B., Thines, N. J., & Elias, B. A. (2006). Nutritional requirements and diet choices of the pygmy rabbit (*Brachylagus idahoensis*): A sagebrush specialist. *Journal of Chemical Ecology*, 32(11), 2455–2474. <https://doi.org/10.1007/s10886-006-9156-2>

Silliman, K. (2019). Population structure, genetic connectivity, and adaptation in the Olympia oyster (*Ostrea lurida*) along the west coast of North America. *Evolutionary Applications*, 12(5), 923–939.

Silva-Brandão, K. L., Horikoshi, R. J., Bernardi, D., Omoto, C., Figueira, A., & Brandão, M. M. (2017). Transcript expression plasticity as a response to alternative larval host plants in the speciation process of corn and rice strains of *Spodoptera frugiperda*. *BMC Genomics*, 18(1), 792. <https://doi.org/10.1186/s12864-017-4170-z>

Sork, V. L., Aitken, S. N., Dyer, R. J., Eckert, A. J., Legendre, P., & Neale, D. B. (2013). Putting the landscape into the genomics of trees: Approaches for understanding local adaptation and population responses to changing climate. *Tree Genetics & Genomes*, 9(4), 901–911. <https://doi.org/10.1007/s11295-013-0596-x>

Sork, V. L., Davis, F. W., Westfall, R., Flint, A., Ikegami, M., Wang, H., & Grivet, D. (2010). Gene movement and genetic association with regional climate gradients in California valley oak (*Quercus lobata* Nee) in the face of climate change. *Molecular Ecology*, 19(17), 3806–3823. <https://doi.org/10.1111/j.1365-294X.2010.04726.x>

Sork, V. L., Squire, K., Gugger, P. F., Steele, S. E., Levy, E. D., & Eckert, A. J. (2016). Landscape genomic analysis of candidate genes for climate adaptation in a California endemic oak, *Quercus lobata*. *American Journal of Botany*, 103(1), 33–46. <https://doi.org/10.3732/ajb.1500162>

Stearns, S. C. (1992). *The evolution of life histories*. Oxford University Press.

Stiebens, V. A., Merino, S. E., Roder, C., Chain, F. J., Lee, P. L., & Eizaguirre, C. (2013). Living on the edge: How philopatry maintains adaptive potential. *Proceedings of the Royal Society B: Biological Sciences*, 280(1763), 20130305. <https://doi.org/10.1098/rspb.2013.0305>

Sultan, S. E., & Spencer, H. G. (2002). Metapopulation structure favors plasticity over local adaptation. *The American Naturalist*, 160(2), 271–283. <https://doi.org/10.1086/341015>

Templeton, A. R., Shaw, K., Routman, E., & Davis, S. K. (1990). The genetic consequences of habitat fragmentation. *Annals of the Missouri Botanical Garden*, 77(1), 13–27. <https://doi.org/10.2307/2399621>

Tigano, A., & Friesen, V. L. (2016). Genomics of local adaptation with gene flow. *Molecular Ecology*, 25(10), 2144–2164. <https://doi.org/10.1111/mec.13606>

Vekemans, X., & Hardy, O. J. (2004). New insights from fine-scale spatial genetic structure analyses in plant populations. *Molecular Ecology*, 13(4), 921–935. <https://doi.org/10.1046/j.1365-294X.2004.02076.x>

Warheit, K. (2001). Genetic diversity and population differentiation of pygmy rabbits (*Brachylagus idahoensis*). Washington Department of Fish and Wildlife, Olympia.

Weiss, N. T., & Verts, B. (1984). Habitat and distribution of pygmy rabbits (*Sylvilagus idahoensis*) in Oregon. *The Great Basin Naturalist*, 44, 563–571.

White, S. M., Flinders, J. T., & Welch, B. L. (1982). Preference of pygmy rabbits (*Brachylagus idahoensis*) for various populations of big sagebrush (*Artemisia tridentata*). *Journal of Range Management*, 35(6), 724–726. <https://doi.org/10.2307/3898249>

Xuereb, A., Kimber, C. M., Curtis, J. M., Bernatchez, L., & Fortin, M. J. (2018). Putatively adaptive genetic variation in the giant California sea cucumber (*Parastichopus californicus*) as revealed by environmental association analysis of restriction-site associated DNA sequencing data. *Molecular Ecology*, 27(24), 5035–5048.

Young, A., Boyle, T., & Brown, T. (1996). The population genetic consequences of habitat fragmentation for plants. *Trends in Ecology & Evolution*, 11(10), 413–418. [https://doi.org/10.1016/0169-5347\(96\)10045-8](https://doi.org/10.1016/0169-5347(96)10045-8)

Zeoli, L. F., Sayler, R. D., & Wielgus, R. (2008). Population viability analysis for captive breeding and reintroduction of the endangered Columbia basin pygmy rabbit. *Animal Conservation*, 11(6), 504–512. <https://doi.org/10.1111/j.1469-1795.2008.00208.x>

Zimmerman, S. J., Aldridge, C. L., Oh, K. P., Cornman, R. S., & Oyler-McCance, S. J. (2019). Signatures of adaptive divergence among populations of an avian species of conservation concern. *Evolutionary Applications*, 12(8), 1661–1677. <https://doi.org/10.1111/eva.12825>

## SUPPORTING INFORMATION

Additional supporting information may be found online in the Supporting Information section.

**How to cite this article:** Byer, N. W., Holding, M. L., Crowell, M. M., Pierson, T. W., Dilts, T. E., Larrucea, E. S., Shoemaker, K. T., & Matocq, M. D. (2021). Adaptive divergence despite low effective population size in a peripherally isolated population of the pygmy rabbit, *Brachylagus idahoensis*. *Molecular Ecology*, 30, 4173–4188. <https://doi.org/10.1111/mec.16040>